PRAMANA
— journal of
physics

© Indian Academy of Sciences

Vol. 64, No. 6
June 2005
pp. 1019–1027

Droplet dynamics on patterned substrates

A DUPUIS and J M YEOMANS
The Rudolf Peierls Centre for Theoretical Physics, University of Oxford,
1 Keble Road, Oxford OX1 3NP, UK
E-mail: yeomans@thphys.ox.ac.uk

Abstract. We present a lattice Boltzmann algorithm which can be used to explore the spreading of droplets on chemically and topologically patterned substrates. As an example we use the method to show that the final configuration of a drop on a substrate comprising hydrophobic and hydrophilic stripes can depend sensitively on the dynamical pathway by which the state is reached. We also consider a substrate covered with micron-scale posts and investigate how this can lead to superhydrophobic behaviour. Finally we model how a Namibian desert beetle collects water from the wind.

Keywords. Droplet spreading; lattice Boltzmann model; patterned surfaces.

PACS Nos 68.08.Bc; 47.11.+j; 83.85.Pt; 61.30.Hn

1. Introduction

A droplet in contact with a substrate will try to spread to an equilibrium shape determined by a balance of surface tensions. This shape, and the droplet's ability to reach it, will be affected by any chemical or topological heterogeneities on the surface. Until recently such disorder was usually regarded as a nuisance. However, with the advent of microfabrication techniques it has become possible to control the chemical or topological patterning of a surface on micron length scales, leading to the possibility of exploring new physics and to novel applications.

An interesting natural example is the Namibian desert beetle which collects water on its back from a fog-laden wind [1]. The beetle's back is bumpy and covered with alternating hydrophobic and hydrophilic regions. Large drops of water condense onto the hydrophilic bumps. The size of the drops then allows them to roll against the wind into the beetle's mouth.

A second example is the lotus leaf which has a surface covered with microscale asperities. These lead to the leaf being superhydrophobic and allow it to shed water droplets easily.

Increasingly, ink-jet printing is becoming an important technique, not only for producing images, but also for device design. For example circuits can be printed using a polymer ink [2], three-dimensional structures can be built up from successive printed layers [3]. The droplets involved in printing typically have length scales of

tens of microns and it is important to understand how their spreading depends on the properties of the substrate onto which they are printed. Experimental work on such mesoscopic drops is difficult and expensive because of the length and time scales involved. Therefore there is a need for numerical modelling both to investigate the underlying physics and to help design the experiments.

Therefore in this paper we describe a lattice Boltzmann algorithm which can be used to investigate the dynamics of droplets evolving on patterned substrates. Lattice Boltzmann is a particularly appropriate approach in that it solves the Navier–Stokes equations but also inputs the thermodynamics information, such as the surface tensions and wetting angles, needed to describe the droplet behaviour.

In §2 we summarise the algorithm and, in particular, the boundary conditions needed to correctly impose a chosen contact angle at the surfaces. Section 3 shows results for surfaces patterned with alternate hydrophobic and hydrophilic stripes. We find that the final droplet shape depends on the point at which the drop impacts the substrate. In §4, we show how the algorithm can be used to handle surfaces with topological patterning and, in particular, to reproduce superhydrophobic behaviour. A simulation reproducing the way a Namibian desert beetle collects water on its back is presented in §5. This is a lovely example combining both chemical and topological patterning.

2. The lattice Boltzmann algorithm

2.1 *Thermodynamics*

We consider a liquid–gas system of density $n(\mathbf{r})$ and volume V. The surface of the substrate is denoted by S. The equilibrium properties are described by the free energy

$$\Psi = \int_V \left(\psi_{\mathrm{b}}(n) + \frac{\kappa}{2} \left(\partial_\alpha n\right)^2 \right) \mathrm{d}V + \int_S \psi_{\mathrm{c}}(n)\, \mathrm{d}S. \tag{1}$$

$\psi_{\mathrm{b}}(n)$ is the free energy in the bulk. We choose a van der Waals form

$$\psi_{\mathrm{b}}(n) = p_{\mathrm{c}} \left(\nu_n + 1\right)^2 \left(\nu_n^2 - 2\nu_n + 3 - 2\beta\tau_w\right), \tag{2}$$

where $\nu_n = (n - n_{\mathrm{c}})/n_{\mathrm{c}}$, $\tau_w = (T_{\mathrm{c}} - T)/T_{\mathrm{c}}$ and $p_{\mathrm{c}} = 1/8$, $n_{\mathrm{c}} = 7/2$ and $T_{\mathrm{c}} = 4/7$ are the critical pressure, density and temperature respectively and β is a constant typically equal to 0.1. The bulk pressure

$$p_{\mathrm{b}} = p_{\mathrm{c}}(\nu_n + 1)^2(3\nu_n^2 - 2\nu_n + 1 - 2\beta\tau_w). \tag{3}$$

The derivative term in eq. (1) models the free energy associated with an interface. κ is related to the surface tension. $\psi_{\mathrm{c}}(n_s) = \phi_0 - \phi_1 n_s + \cdots$ is the Cahn surface free energy [4] which controls the wetting properties of the fluid.

The lattice Boltzmann algorithm solves the Navier–Stokes equations for this system. Because interfaces appear naturally within the model it is particularly well-suited for looking at the behaviour of moving drops.

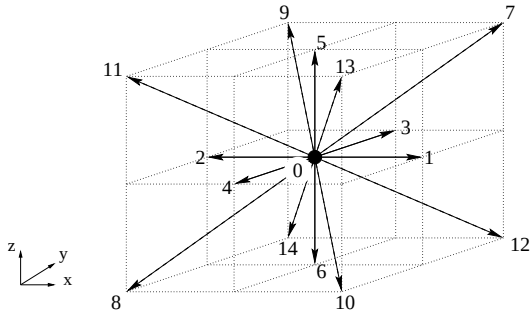

Figure 1. Topology of a $D3Q15$ lattice. The directions i are numbered and correspond to the velocity vector $\mathbf{v_i}$.

2.2 *The numerical scheme*

The lattice Boltzmann approach follows the evolution of partial distribution functions f_i on a regular, d-dimensional lattice formed of sites $\mathbf{r}$. The label i denotes velocity directions and runs between 0 and z. $DdQz+1$ is a standard lattice topology classification. The $D3Q15$ lattice we use here has the following velocity vectors $\mathbf{v_i}$: $(0,0,0)$, $(\pm1,\pm1,\pm1)$, $(\pm1,0,0)$, $(0,\pm1,0)$, $(0,0,\pm1)$ in lattice units as shown in figure 1. The lattice Boltzmann dynamics are given by

$$f_i(\mathbf{r}+\Delta t\mathbf{v_i}, t+\Delta t) = f_i(\mathbf{r},t) + \frac{1}{\tau}\left(f_i^{\mathrm{eq}}(\mathbf{r},t) - f_i(\mathbf{r},t)\right), \tag{4}$$

where Δt is the time step of the simulation, τ the relaxation time, and f_i^{eq} the equilibrium distribution function which is a function of the density $n = \sum_{i=0}^{z} f_i$ and the fluid velocity $\mathbf{u}$, defined through the relation

$$n\mathbf{u} = \sum_{i=0}^{z} f_i \mathbf{v_i}. \tag{5}$$

The relaxation time tunes the kinematic viscosity as [5]

$$\nu = \frac{\Delta\mathbf{r}^2}{\Delta t}\frac{C_4}{C_2}\left(\tau - \frac{1}{2}\right), \tag{6}$$

where $\Delta\mathbf{r}$ is the lattice spacing and C_2 and C_4 are coefficients related to the topology of the lattice. These are equal to 3 and 1 respectively when one considers a $D3Q15$ lattice.

It can be shown [6] that eq. (4) reproduces the Navier–Stokes equations of a non-ideal gas if the local equilibrium functions are chosen as

$$\begin{aligned} f_i^{\mathrm{eq}} &= A_\sigma + B_\sigma u_\alpha v_{i\alpha} + C_\sigma \mathbf{u}^2 + D_\sigma u_\alpha u_\beta v_{i\alpha} v_{i\beta} + G_{\sigma\alpha\beta} v_{i\alpha} v_{i\beta},\ i>0, \\ f_0^{\mathrm{eq}} &= n - \sum_{i=1}^{z} f_i^{\mathrm{eq}}, \end{aligned} \tag{7}$$

where Einstein notation is understood for the Cartesian labels α and β and where σ labels velocities of different magnitude. A possible choice of the coefficients is [7]

$$A_\sigma = \frac{w_\sigma}{c^2}\left(p_\mathrm{b} - \frac{\kappa}{2}(\partial_\alpha n)^2 - \kappa n \partial_{\alpha\alpha} n + \nu u_\alpha \partial_\alpha n\right),$$

$$B_\sigma = \frac{w_\sigma n}{c^2}, \quad C_\sigma = -\frac{w_\sigma n}{2c^2}, \quad D_\sigma = \frac{3w_\sigma n}{2c^4},$$

$$G_{1\gamma\gamma} = \frac{1}{2c^4}\left(\kappa(\partial_\gamma n)^2 + 2\nu u_\gamma \partial_\gamma n\right), \quad G_{2\gamma\gamma} = 0,$$

$$G_{2\gamma\delta} = \frac{1}{16c^4}\left(\kappa(\partial_\gamma n)(\partial_\delta n) + \nu(u_\gamma \partial_\delta n + u_\delta \partial_\gamma n)\right), \tag{8}$$

where $w_1 = 1/3$, $w_2 = 1/24$ and $c = \Delta\mathbf{r}/\Delta t$.

2.3 *Wetting boundary conditions*

The major new challenge in dealing with patterned substrates is to handle the wetting boundary conditions correctly. For flat substrates a boundary condition can be established by minimising the free energy (1) [4]

$$\hat{\mathbf{s}} \cdot \nabla n = -\frac{\phi_1}{\kappa}, \tag{9}$$

where $\hat{\mathbf{s}}$ is the unit vector normal to the substrate. It is possible to obtain an expression relating ϕ_1 to the contact angle θ as [8]

$$\phi_1 = 2\beta\tau_w\sqrt{2p_\mathrm{c}\kappa}\ \mathrm{sign}\left(\frac{\pi}{2} - \theta\right)\sqrt{\cos\frac{\alpha}{3}\left(1 - \cos\frac{\alpha}{3}\right)}, \tag{10}$$

where $\alpha = \cos^{-1}(\sin^2\theta)$ and the function sign returns the sign of its argument.

Equation (9) is used to constrain the density derivative for sites on a flat part of the substrate. However, no such exact results are available for sites at edges or corners. We work on the principle that the wetting angle at such sites should be constrained as little as possible so that, in the limit of an increasingly fine mesh, it is determined by the contact angle of the neighbouring flat surfaces. Details can be found in [9,10].

Finally we note that the usual no-slip boundary condition is imposed on the velocity [7].

3. Chemical patterning

As an example of chemical patterning we consider surfaces formed by alternating hydrophobic and hydrophilic stripes. Figure 2 shows such a substrate, where hydrophilic stripes, which correspond to a contact angle 5° are shown in dark grey

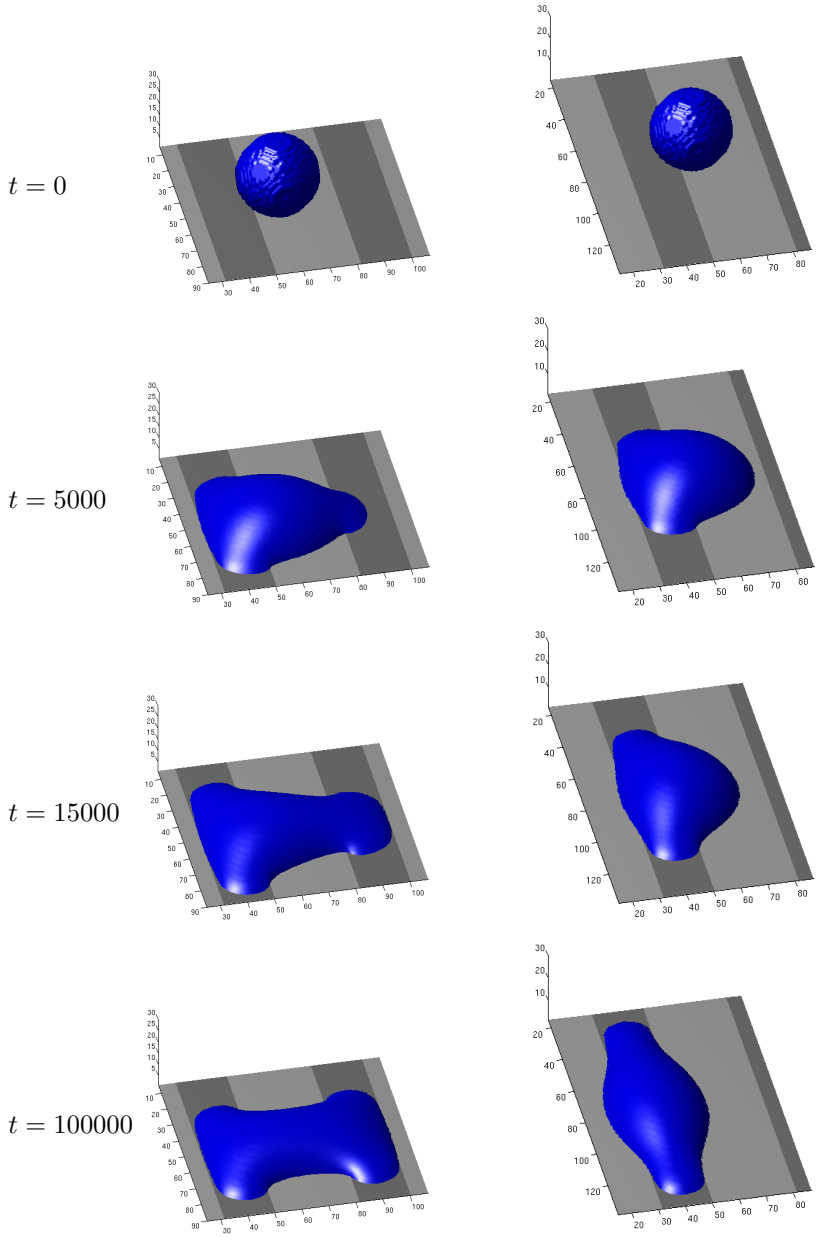

Figure 2. Droplet spreading on a chemically striped surface. Hydrophilic and hydrophobic stripes appear dark and pale respectively. (**a**) The point of impact is closer to the hydrophobic stripe center. (**b**) It is closer to the stripe boundary. The other parameters are identical in (a) and (b).

and hydrophilic stripes which correspond to a contact angle 64° are shown in light grey. The ratio of stripe widths is 4 : 7.

The figure shows, top to bottom, the time evolution of a drop jetted on the substrate. The only difference between the left-hand and right-hand sequences in the figure is the initial point of contact: it is apparent that changing this can lead to a very different final state. If the drop lands close to mid-way between two hydrophilic stripes, and is able to reach both of them as it spreads, its final shape is a butterfly-like configuration. If, however, it lands sufficiently close to one stripe that it never reaches the neighbouring stripe it prefers to lie predominantly on a single hydrophilic stripe. Both final configurations have similar free energies, however the global equilibrium is the butterfly shape. These equilibrium shapes were found to quantitatively match experiments [11]. The final configuration is also influenced by the jetting velocity [11]: as expected a higher impact velocity favours the butterfly configuration.

The following lattice Boltzmann parameters were used. The initial droplet radius $R_0 = 30$ lattice sites. The droplet was initialised with a vertical velocity equal to $U_0 = 0.02$. The lattice geometry was $L_x \times L_y \times L_z$ where L_x and L_y were chosen large enough to not affect the behaviour of the droplet and $L_z = 40$. The relaxation time $\tau = 0.63$. The surface tension related parameter $\kappa = 0.0012$. The temperature $T = 0.4$ which leads to two phases of density $n_\mathrm{l} = 4.128$ and $n_\mathrm{g} = 2.913$. The simulations were run for 400,000 iterations. If these values are mapped onto the physical viscosity, surface tension and density of water then the drop sizes are of the order of microns.

4. Topological patterning

We now apply the algorithm to topological patterning in order to reproduce the superhydrophobic behaviour of a drop on a substrate patterned by square posts.

Figure 3 shows the final state attained by the droplet for different substrates and initial conditions. For comparison, figure 3a shows a planar substrate. The equilibrium contact angle is $\theta_a = 110^\mathrm{o} = \theta_\mathrm{input}$ as expected [7]. In figure 3b the substrate is patterned and the initial velocity of the drop is zero. Now the contact angle is $\theta_\mathrm{b} = 156^\mathrm{o}$, a demonstration of superhydrophobic behaviour. Figure 3c reports an identical geometry but a drop with an initial impact velocity. Now the drop is able to collapse onto the substrate and the final angle is $\theta_\mathrm{b} = 130^\mathrm{o}$. These angles are compatible with the ones reported in [12] where similar parameters are considered.

For the parameter values used in these simulations the state with the droplet suspended on the posts has a slightly higher free energy than the collapsed state. The suspended state is a metastable state but the droplet, with diameters smaller than the capillary length, needs an impact velocity to reach the true thermodynamic ground state. For macroscopic drops gravity will also be important in determining whether the drop remains suspended on top of the posts [13].

The size of the domain is $L_x \times L_y \times L_z = 80 \times 80 \times 80$ and the height, spacing and width of posts are $h = 5$, $d = 8$ and $w = 4$ respectively. A spherical droplet of radius $R = 30$ is initially centered around the point $(x; y; z) = (41; 41; 36)$. The

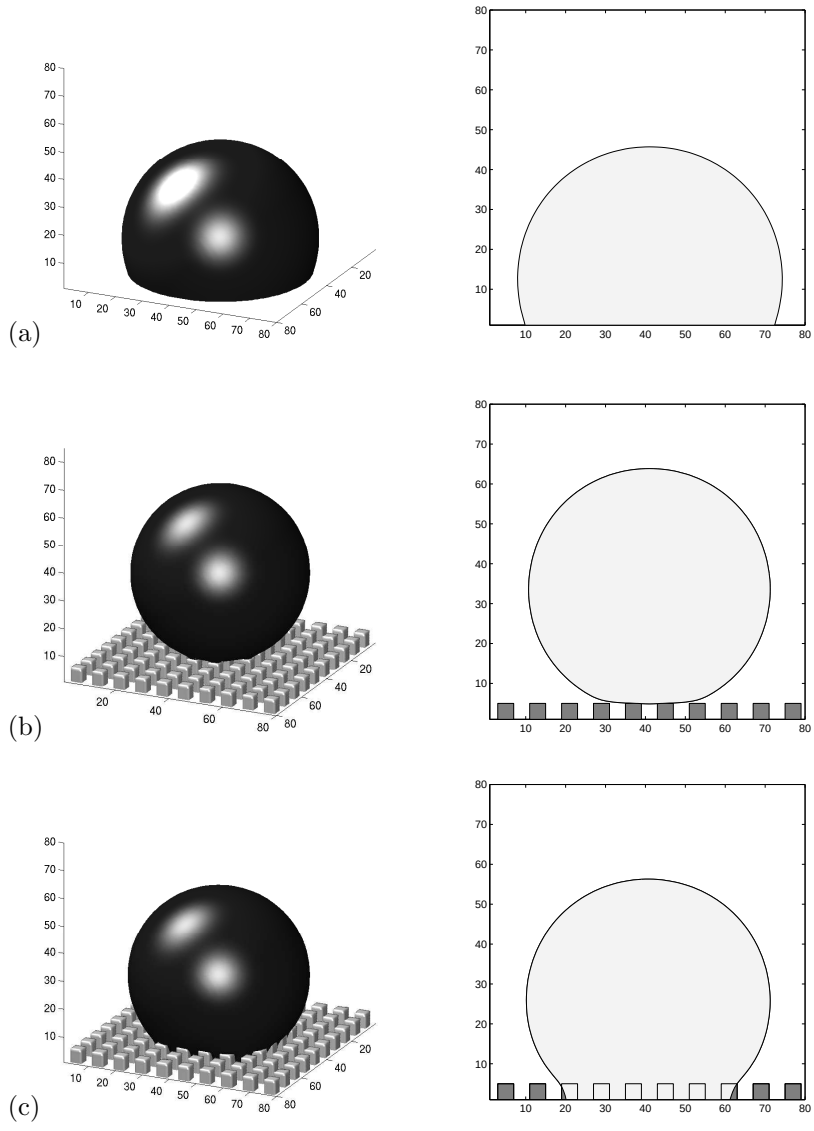

Figure 3. Final states of a spreading droplet. The right column reports cuts at $y = 41$. (**a**) The substrate is flat and homogeneous. (**b**) The substrate is decorated with posts and the initial velocity of the droplet is 0. (**c**) Same geometry as (b) but the droplet reaches the substrate with a velocity $0.01\Delta\mathbf{r}/\Delta t$. Each of these simulations ran for approximately 8 h on eight processors on a PC cluster.

contact angle $\theta_{\text{input}} = 110^{\text{o}}$ is set on every substrate site. The surface tension and the viscosity are tuned by choosing parameters $\kappa = 0.002$ and $\tau = 0.8$ respectively. The liquid density n_{l} and gas density n_{g} are set to $n_{\text{l}} = 4.128$ and $n_{\text{g}} = 2.913$ and the temperature $T = 0.4$. Gravity is not considered.

5. Water capture by a desert beetle

As an example combining both chemical and topological patterning, we consider the process by which a beetle species living in the Namibian desert collect drinking water on its back from a fog-laden wind [1].

The beetle's back is covered by tiny peaks of diameter ~ 0.5 mm. The whole structure except the top of the peaks is coated in wax which forms a bumpy hydrophobic surface, whereas the top of the peaks are hydrophilic.

By tilting its body forward into the wind, the beetle collects water from dense fog. The water condenses into droplets which settle at the top of the peaks. Once the droplets collected are large enough they spread beyond the peaks and may eventually coalesce with a neighbour to form a larger drop. This drop is then heavy enough to roll downwards against the wind to reach the mouth of the beetle.

We demonstrate the ability of our model to deal with patterned substrates by considering a domain of size $L_x \times L_y \times L_z = 50 \times 50 \times 30$ covered by four $l_x \times l_y \times l_z = 10 \times 10 \times 5$ peaks. The minimum distance between the centers of the peaks is 20. The equilibrium contact angle is set to 70° on every surface site apart for those located at the top of the peaks where it is equal to 35°. The surface tension and the viscosity are tuned by choosing parameters $\kappa = 0.002$ and $\tau = 0.8$ respectively. The liquid density n_l and gas density n_g are set to $n_l = 4.128$ and $n_g = 2.913$ and the temperature $T = 0.4$. The system is initialised with a gas density greater than the equilibrium value ($n_g^0 = 3.07$) and a body force $\mathbf{G} = (0, 0, 8 \cdot 10^{-8})$ is imposed to play the role of gravity.

Simulation results are presented in figure 4. Fluid initially condenses at the top of the peaks because of their hydrophilic nature. Due to the high water saturation, the droplets continue to spread beyond the hydrophilic area until they coalesce to

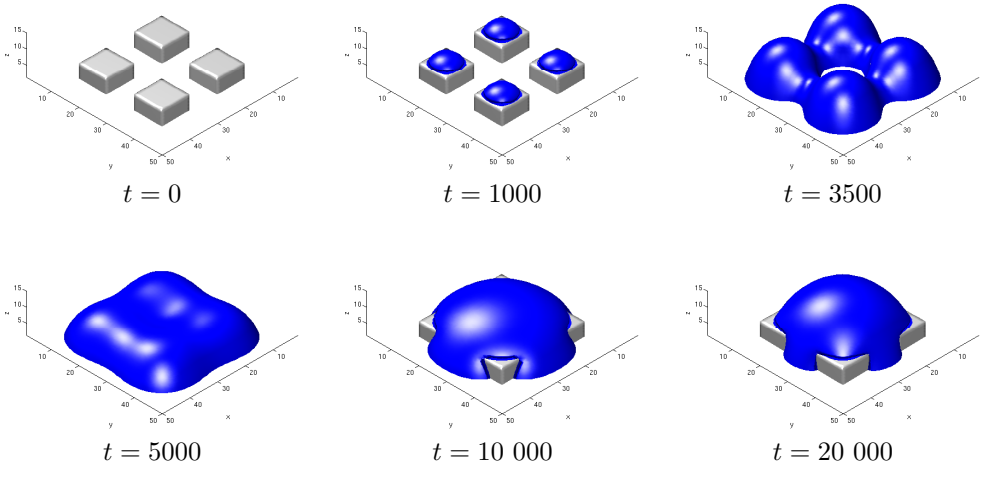

Figure 4. Fog condensing on a beetle's back. The top of the posts are hydrophilic, the remainder of the substrate is hydrophobic. t labels the time in simulation units.

form a bumpy ring. Surface tension causes the ring to shrink and eventually to form a single droplet which may be sufficiently large to roll into the wind to reach the beetle's mouth.

6. Conclusions

We have described a lattice Boltzmann model able to follow the behaviour of drops spreading on topologically and chemically patterned substrates. The algorithm gives us the capability to explore a wide variety of droplet behaviours on novel substrates and in microfluidic devices. For example, we are interested in gaining a greater understanding of how drops move across superhydrophobic surfaces [9]. Moreover there is interesting work to be done exploring the dynamics of wetting in wedges.

Acknowledgements

Supercomputing resources were provided by the Oxford Supercomputing Centre. AD acknowledges the support of the EC IMAGE-IN project GR1D-CT-2002-00663.

References

[1] A R Parler and C R Lawrence, *Nature (London)* **414**, 33 (2001)
[2] H Sirringhaus, T Kawase, R H Friend, T Shimoda, M Inbasekaran, W Wu and E P Woo, *Science* **290**, 2123 (2000)
[3] K E Cooke, M Bamber, J Bassas, D Boscarino, B Derby, A Figueras, B J Inkson, V Rigato, T Steer and D G Teer, *Surf. Coat. Tech.* **162**, 276 (2003)
[4] J W Cahn, *J. Chem. Phys.* **66**, 3667 (1977)
[5] S Succi, *The lattice Boltzmann equation, for fluid dynamics and beyond* (Oxford University Press, 2001)
[6] M R Swift, E Orlandini, W R Osborn and J M Yeomans, *Phys. Rev.* **E54**, 5051 (1996)
[7] A Dupuis and J M Yeomans, *Fut. Gen. Comp. Syst.* **20**, 993 (2004)
[8] A J Briant, P Papatzacos and J M Yeomans, *Philos. Trans. R. Soc. London, Ser. A* **360**, 485 (2002)
[9] A Dupuis and J M Yeomans, Mesoscopic modelling of droplets on topologically patterned substrates, in: *Proceedings of the ICCS 2004 conference* edited by P M A Sloot *et al* (Springer, 2004). vol. 3039 of LNCS, pp. 556–563, available at http://xxx.lanl.gov/cond-mat/0401150
A Dupuis and J M Yeomans, *Langmuir* **21**, 2624 (2005)
[10] A Dupuis and J M Yeomans, Droplets on patterned substrates: Water off a beetle's back, *Int. J. Numer. Meth. Fluids* (2004) submitted
[11] J Léopoldès, A Dupuis, D G Bucknall and J M Yeomans, *Langmuir* **19**, 9818 (2003)
[12] D Öner and T J McCarthy, *Langmuir* **16**, 7777 (2000)
[13] C W Extrand, *Langmuir* **18**, 7991 (2002)